Turk J Phys
35 (2011) , 137 – 143.
© TÜBİTAK
doi:10.3906/fiz-1012-58

Resonant transfer excitation followed by X-ray for boron-like ions

Hassan RAMADAN
Basic Sciences Department, Faculty of Computer and Information Sciences,
Ain Shams University, Cairo-EGYPT
e-mail: hramadan@eun.eg

Received: 07.12.2010

Abstract

Theoretical cross sections for resonant transfer excitation followed by x-ray emission (RTEX) are calculated for the collisions of some ions in the series of the Boron-like ions with H_2 as a target. The calculations have been done for C II, N III, O IV, F V, Ar XIV and Fe XXII ions by folding their dielectronic recombination (DR) cross sections over the momentum distribution (Compton profile) of H_2 target gas. Calculations have been performed from both ground and metastable initial states, in LS - coupling, allowing for $\triangle n = 0$ excitations.

In the present work, the RTEX cross sections of the ions C II, N III, O IV and F V exhibit one peak behavior, but shows two overlapped peaks in case of Ar XIV ion. RTEX cross section gives two separated peaks for Fe XXII ion. It is expected that the new results would lead to a revision of the spectral diagnostics of the B-like ions in laboratory and astrophysical sources, in particular the x-ray spectra observed from solar flares and tokamaks.

Key Words: Transition probability, resonant transfer excitation

1. Introduction

Interference effects in resonant transfer excitation (RTE) can be studied for low Z projectiles via Auger electrons emitted from highly ionized fast moving projectile ions following collisions with low Z targets. RTE in ion-atom collisions is closely related to dielectronic recombination. In the latter case, which is of practical interest to the fusion power program, an electron with the proper velocity incident on a highly charged ion is resonantly captured and simultaneously interacts with an inner shell electron to excite it, thus forming a doubly excited state which may decay predominantly via x-ray emission (RTEX) for higher Z ions or by Auger electron decay (RTEA) for lower Z ions. The resonant velocity is that of the Auger electron emitted by the ion in the doubly excited state. In RTE, the electrons to be captured are in low Z atomic (typically He) or Molecular (typically H_2) targets and the ions are produced by accelerators in highly charged states with the appropriate resonant velocity. The resonance is much broadened by the velocity distribution of the target electrons. Thus, the resonance width as a function of projectile energy is determined by folding the Compton profile of the target electrons with the dielectronic recombination cross sections.

Boron-like ions are present in a variety of astrophysical objects such as the planetary nebulae, novae, Seyfert galaxies, the interstellar medium and the Sun. Thus, accurate atomic data is needed not only for the spectral diagnostics of laboratory plasmas but also for the diagnostics of these important astrophysical objects.

Since the pioneering work by Burgess [1, 2], much effort has been spent, both theoretically and experimentally, to obtain accurate dielectronic recombination rate coefficients for many atomic ions. Results of many of these studies have been summarized and compiled by a number of workers [3–5]. Dielectronic recombination rate coefficients for Fe XXII were calculated by Badnell [6] and Zhang [7] using a multi-configuration LS -coupling expansion, allowing for $\triangle n = 0$ and $\triangle n = 1$ core-excitations, at temperatures between 105 K and 109 K. Badnell and Pindzola [8] have carried-out LS-coupling and intermediate coupling calculations for dielectronic recombination rate coefficients of C II, N III, and O IV ions, between 104 K and 107 K, allowing only for $\triangle n = 0$ core-excitations from the ground state. Dielectronic recombination cross sections for N III, O IV and F V were estimated by Nasser and Hahn [9] using single configuration non-relativistic Hartree-Fock wave functions in LS-coupling, over an incident electron energies ranging from 0.07 Ry to 1.15 Ry. Badnell [10] have calculated energy-averaged dielectronic recombination cross sections in LS -coupling from the ground and metastable initial states of OIII and F V ions, as a function of electron energy ranging from 0 eV to 25 eV. There was an early calculation on C II by LaGattuta and Hahn [11] in LS -coupling in the range of 9.0 eV to 9.3 eV using LS term-averaged Hartree-Fock single-particle states in a frozen-core approximation. No results were found for the RTEX cross sections for these ions.

So, in the present paper, The RTEX cross sections for C II, N III, O IV, F V, Ar XIV and Fe XXII in collision with the light target (hydrogen) are considered. The calculations were carried out in impulse approximation.

2. Theory

The work presented in this paper is considered for a series of calculations of the RTEX cross sections of the initial ions which are members of Boron isoelectronic sequence. In particular, the target ions C II, N III, O IV, F V, Ar XIV and Fe XXII are examined at low energies and undergo the initial excitation capture

$$\underset{\text{(i)}}{1s^2 2s^2 2p + \ell_c e_c} \quad \rightarrow \underset{\text{(d)}}{1s^2 2s 2p^2 n\ell(\triangle n_t = 0)}, \tag{1}$$

with 2s→2p and $n_t = 2$. This is followed by a radiative decay

$$\begin{array}{lll} 1s^2 2s 2p^2 n\ell & \rightarrow 1s^2 2s^2 2pn\ell & + \gamma(2p \rightarrow 2s) \\ & \rightarrow 1s^2 2s 2p^2 n'\ell' & + \gamma(n\ell \rightarrow n'\ell') \\ \text{(d)} & \text{(f)} & \end{array}$$

The initial state has the multi-electron configuration ^{2}P, which may be put in the form $1s^2 2s^2 2p[^2P] + \ell_c e_c$. The intermediate states $1s^2 2s 2p^2 n\ell$ are more complex than the initial state, since there is just one electron in 2s orbit and two electrons in 2p orbit. The multi-electron configurations are of the forms ^{2}S, ^{2}P, ^{2}D, and ^{4}P. By arranging the energies of these states, it is found that the ^{2}P state has the highest energy followed by

^{2}S, ^{2}D, and ^{4}P, respectively. Accordingly, there will be four classes of Auger channels A, B, C, and D. Class A occurs for those intermediate states of only one Auger channel, e.g. (^{4}P→ $^2\bar{P}$), etc. Class B occur for those intermediate states of two Auger channels, e.g. (^{2}D→ $^2\bar{P}$) and (^{2}D→ ^{4}P) , etc. Class C occurs for those intermediate states of three Auger channels e.g. (^{2}S→ $^2\bar{P}$), (^{2}S→ ^{4}P) and (^{2}S→ ^{2}D), etc. Class D occurs for those intermediate states of four Auger channels e.g. (^{2}P→ $^2\bar{P}$), (^{2}P→ ^{4}P), (^{2}P→ ^{2}D), and (^{2}P→ ^{2}S), etc.

There are several possible modes of excitation for the initial state $i = 1s^2 2s^2 2p$. The 2p electron may be excited to $n_a \geq 3$ as $i + e_c\ell_c \to 1s^2 2s^2 n_a\ell_a n\ell$. The 2s electron may be excited to either 2p or $n_a \geq 3$. And the 1s electron may be elevated to excitation.

In the following, the projectile energy e_c is limited to the low energy region such that only 2s → 2p excitation of (1), where this mode ($\triangle n_t = 0$) is often dominant for low Z ions, and at low temperatures.

The nonrelativistic Hartree-Fock wave functions and LS coupling are employed in evaluating the necessary amplitudes. The intermediate states $|d\rangle$ are considered by

$$|d\rangle = |((1s^2 2s, 2p^2(L_a S_a))L_t S_t, n\ell)LS\rangle, \ \ (L_a = L_t), \tag{2}$$

where the initial ground states

$$|i\rangle = |((1s^2 2s 2p^2)L_t S_t, e_c\ell_c)LS\rangle, \ \ \equiv i_1, \ \ \text{with} \ \ L_t = 1, S_t = 1/2; \tag{3}$$

and the metastable initial state with $S_t = 3/2$,

$$|i'\rangle = |((1s^2 2s 2p^2(L_a S_a))(L_t = 1, S_t = 3/2), e'_c\ell'_c)LS\rangle. \tag{4}$$

The following formula for the cross section is used:

$$\bar{\sigma}^{DR} = [\frac{4\pi}{(p_0 a_0)^2}](\frac{Ry}{\triangle e_c})[\tau_0 V_a(i \to d)]\omega(d)(\pi(a_0)^2), \tag{5}$$

where p_0 is the momentum of the free electron, a_0 is Bohr radius, τ_0 is the atomic unit of time which is given as $\tau_0 = 2.4189 \times 10^{-17}$ s, and $V_a(i \to\to d)$ and $\omega(d)$ are the radiationless capture probability and fluorescence yield respectively given by

$$V_a(i \to\to d) = \left(\frac{g_d}{2g_i}\right) \sum_{i_c,\ell_c} A_a(d \to i_c\ell_c) \tag{6}$$

and

$$\omega(d) = \frac{\sum_f A_r(d \to f)}{\Gamma_a(d) + \Gamma_r(d)}, \tag{7}$$

where $\Gamma_r(d) = \sum_f A_r(d \to f)$, $\Gamma_a(d) = [\sum_{i_c,\ell_c} A_a(d \to i_c\ell_c) + \sum_{j_c,\ell_c} A_a(d \to j_c\ell_c)]$, and the Auger and radiative transition probabilities A$_a$ and A$_r$ are the basic components of the cross section given by the relations

$$\begin{aligned} A_a(d \to i) = g_i \hat{\ell}\hat{\ell}_c^2 \hat{L}_t \hat{S}_t \hat{S}_a \begin{Bmatrix} \ell & L_t & L \\ 1 & \ell_c & 1 \end{Bmatrix} \times \\ \left| \sum_{S=0,1} \hat{S}'' \begin{Bmatrix} 1/2 & S_t & S'' \\ 1/1 & 1/2 & S_a \end{Bmatrix} \begin{Bmatrix} 1/2 & S_t & S'' \\ 1/1 & 1/2 & S \end{Bmatrix} I(\ell_c, S'') \right|^2, \end{aligned} \tag{8}$$

where,

$$\begin{aligned} I(L_{ab},S_{ab}) = \textstyle\sum_K R_K(\ell_S\ell_c;\ell_a\ell_b) \begin{pmatrix} \ell_s & K & \ell_a \\ 0 & 0 & 0 \end{pmatrix} \begin{pmatrix} \ell_c & K & \ell_b \\ 0 & 0 & 0 \end{pmatrix} \times \\ \begin{Bmatrix} \ell_s & \ell_a & K \\ \ell_b & \ell_c & L_{ab} \end{Bmatrix} \\ +(-)^{L_{ab}-S_{ab}} \textstyle\sum_{K'} R_{K'}(\ell_s\ell_c;\ell_b\ell_a) \begin{pmatrix} \ell_s & K' & \ell_b \\ 0 & 0 & 0 \end{pmatrix} \begin{pmatrix} \ell_c & K' & \ell_a \\ 0 & 0 & 0 \end{pmatrix} \times \\ \begin{Bmatrix} \ell_s & \ell_b & K' \\ \ell_a & \ell_c & L_{ab} \end{Bmatrix}, \end{aligned} \tag{9}$$

where R_K is the usual radial integral.

On the other hand, there are three possible radiative decay modes:

$$A_r(d \to f_1 = 2s^2 2pn\ell) = \hat{S}_a A_r^0(2p \to 2s) \tag{10}$$

$$A_r(d \to f_2 = 2s^2 2p^2) = 2A_r^0(n\ell \to 2s) \tag{11}$$

and

$$\begin{aligned} A_r(d \to f_3 = 2s2p^3) = 3\hat{\ell}\hat{S}_t A_r^0(n\ell \to 2p)\times \\ \textstyle\sum_{S;L;} \hat{S}'\hat{L}' \begin{Bmatrix} L_a & 1 & L' \\ 1 & L & \ell \end{Bmatrix}^2 \begin{Bmatrix} 1/2 & S_a & S_t \\ 1/2 & S & S' \end{Bmatrix}^2 \left| G_{L_aS_a}^{L'S'} \right|^2, \end{aligned} \tag{12}$$

where G is known as the fractional parentage coefficients for the $2p^3$ state.

Finally, the RTEX process can be represented schematically as:

$$A^{q+} + B \longrightarrow (A^{(q-1)+})^{**} + B^+ \longrightarrow (A^{(q-1)+})^* + B^+ + \gamma\,. \tag{13}$$

The atom B (H_2 in this paper) in ion-atom collision plays no role in the RTEX process. Since the Compton profile gives the probability of finding a particular target electron with a momentum p_z, it is utiliaed (Hahn [12]) with the impulse approximation (IMA) to relate the RTEX cross section ($\bar{\sigma}^{\mathrm{RTEX}}$) to the DR cross section ($\bar{\sigma}^{\mathrm{DR}}$) (see equation (5)). The relationship between DR and RTEX cross sections, following Hahn [12] and Brandt [13], is given by the relation

$$\bar{\sigma}^{\mathrm{RTEX}} = \sqrt{\frac{M}{2E}} \triangle e_c J_B(p_{\mathrm{z}}) \bar{\sigma}^{\mathrm{DR}} \tag{14}$$

where, M is the mass of the projectile ion of energy E, $J_B(p_{\mathrm{z}})$ is the Compton profile and p_{z} is the z-component of the momentum.

3. Results and discussions

The DR cross sections for the interested ions and the generated RTEX cross sections are calculated using the RCN/RCG code (Cowan) for a more accurate determination of transition energies and transition probabilities.

The discussion will be classified into two groups. The first group (low charging ions) is considered for C II, N III, O IV, and F V, while the second group (highly charged ions) is considered for Ar XIV and Fe XXII.

Since there are too many states to be calculated, the error in each value of A_a and A_r is found to be about 10 percent of the correct results (Hahn [13]).

3.1. Low charging ions

The RTEX cross sections are obtained from their corresponding DR cross sections for the ions C II, N III, O IV, and F V, and is drawn in Figure (1). The σ^{RTEX} shows a one-peak behavior with smallest width and peak value for the C II ion. The width increases from C II to F V. σ^{RTEX} increases with increasing Z of the ions in the B isoelectronic sequence. However, this behavior is changed for F V ion, where the cross section starts to decrease (Table 1).

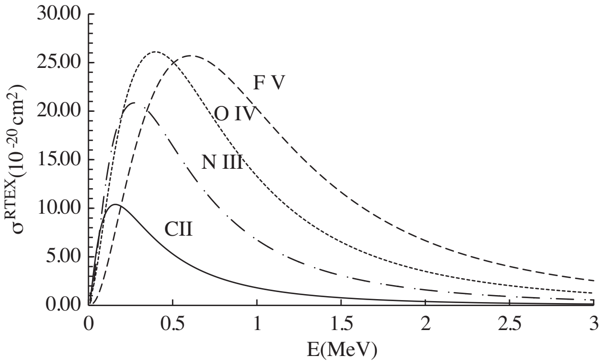

Figure 1. The RTEX cross section, in cm^2, for the collision of CII, NIII, OIV and FV ions with H_2 atom.

Table 1. The Peak values of the RTEX cross sections (in 10^{-20} cm^2) for the collision of the ions.

Ion	E (MeV)	σ^{RTEX}
CII	0.16	10.4
NIII	0.27	20.8
OIV	0.4	26.1
FV	0.61	25.7

3.2. High charging ions

The RTEX cross sections are obtained from their corresponding DR cross sections for the ions Ar XIV and Fe XXII, and drawn in Figure 2. Figure 2 shows that the RTEX cross section has two overlapped peaks in case of Ar XIV and two separated peaks in case of Fe XXII.

Table 2 is considered as a sample of the calculations of the DR cross sections for FeXXII ion in the B isoelectronic sequence at continuum energies $e_c = 8.07$ Ry.

4. Conclusion

The RTEX cross sections for the B-like ions are obtained from the DR cross sections by the method of folding and it is found the following:

- $\bar{\sigma}^{\mathrm{RTEX}}$ exhibits one peak behavior for C II, N III, OIV and F V ions. However, $\bar{\sigma}^{\mathrm{RTEX}}$ for Ar XIV shows two highly overlapped peaks behavior which reflects the nature of DR cross sections at high Z ions.

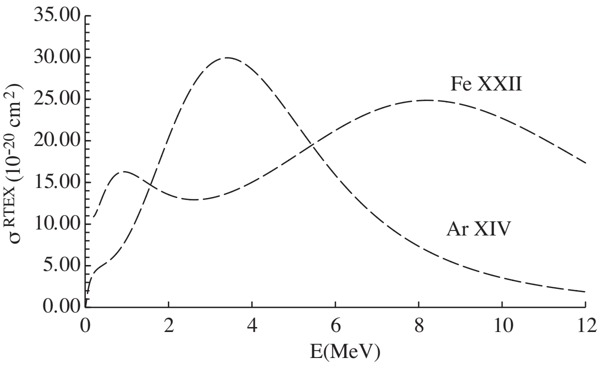

Figure 2. Same as Figure 1, but for the ions ArXIV and FXXII with H_2.

Table 2. The intermediate state $1s^2 2s2p^2[^2P]23d$ of Fe XXII with energy $e_c = 8.07$ Ry, where $A_{a1,2,3,4}$ are the Auger transitions from the intermediate state to $[^2P]$ initial state (i) and to ^4P, ^3D and ^2S ,respectively. $A_{r1,2}$ are the radiative transitions for $^2P \rightarrow {}^2\bar{P}$ and the sum of the rest of the radiative transitions respectively. $\bar{\sigma}^D R$ are given in units of 10^{-20} cm^2. The values of A_a and A_r are in units of sec^{-1}. (The values between parentheses are powers of 10).

L	S	A_{a1}	A_{a2}	A_{a3}	A_{a4}	A_{r1}	A_{r2}	ω	$\bar{\sigma}^{DR}$
1	0	0.381(+12)		0.769(+12)		0.921(+11)	0.291(+10)	0.953(-1)	0.0302
1	1	0.497(+12)	0.438(+12)	0.849(+11)		0.921(+11)	0.493(+11)	0.122(0)	0.154
2	0	0.140(+13)		0.318(+12)	0.623(+12)	0.921(+11)	0.480(+11)	0.564(-1)	0.110
2	1	0.137(+13)	0.107(+12)	0.353(+11)	0.681(+11)	0.921(+11)	0.177(+11)	0.652(-1)	0.370
3	0	0.466(+12)		0.198(+13)		0.921(+11)	0.480(+11)	0.542(-2)	0.0490
3	1	0.204(+12)	0.247(+11)	0.220(+12)		0.921(+11)	0.177(+11)	0.197(0)	0.234
									0.944

- $\bar{\sigma}^{\mathrm{RTEX}}$ for low charging ions collides with H_2 extends between energies of 0.0 MeV–2.0 MeV.
- $\bar{\sigma}^{\mathrm{RTEX}}$ for highly charging ions collides with H_2 extends between energies of 0.0 MeV–12.0 MeV.
- For Ar XIV with $Z = 18$ the RTEX cross section starts to exhibit two overlapped peak behavior.
- For Fe XXII with $Z = 26$ the RTEX cross section exhibits two separated peaks behavior. This two peak behavior causes an apparent drop in the maximum value of RTEX cross section for Fe XXII ion.

References

[1] A. Burgess, *ApJ*, **139**, (1964), 776.

[2] A. Burgess, *ApJ*, **141**, (1965), 1588.

[3] Z. Altun, A. Yumak, N. R. Badnell, J. Colgan and M. S. Pindzola, *A&A*, **420**, (2004), 775.

[4] H. Ramadan and G. Omar, *Sixth Radiation Physics Conference 27-30 Oct., Assiut-Egypt*, (2002), 381. & H. Ramadan, G. Omar and T. El-Kafrawy, *First International Conference on Modern Trends in Physics Research ATPR-04* (American Institute of Physics), (2005), 79.

[5] H. Ramadan and S. Elkilany, *Z. Naturforsch.*, **65a**, (2010), 1.

[6] N. R. Badnell, *J. Phys.*, **B19**, (1986), 3827.

[7] H. L. Zhang and A. K. Pradhan, *Astron. Astrophys. Suppl. Ser.*, **123**, (1997), 575.

[8] N. R. Badnell and M. S. Pindzola, *Phys. Rev.*, **A39**, (1989), 1690.

[9] I. Nasser and Y. Hahn, *Phys. Rev.*, **A 39**, (1989), 401.

[10] N. R. Badnell, M. S. Pindzola, L.H. Andersen, J. Bolko and H.T. Schmidt, *J. Phys.*, **B24**, (1991), 4441.

[11] K. LaGattuta and Y. Hahn, *Phys. Rev Lett.*, **51**, (1983), 558.

[12] Y. Hahn, *Adv. Atom & Molec. Phys.*, **21**, (1985), 123.

[13] D. Brandt, *Phys. Rev.*, **A27**, (1983), 1314.